# Stabilizing Heterobimetallic Complexes Containing Unsupported Ti−M Bonds (M = Fe, Ru, Co): The Nature of Ti−M Donor−Acceptor Bonds

**Stefan Friedrich, Harald Memmler, and Lutz H. Gade***

Institut für Anorganische Chemie, Universität Würzburg, Am Hubland, D-97074 Würzburg, Germany

**Wan-Sheung Li, Ian J. Scowen, and Mary McPartlin**

School of Chemistry, University of North London, Holloway Road, London N7 8DB, U.K.

**Catherine E. Housecroft**

Institut für Anorganische Chemie, Universität Basel, Spitalstrasse 51, CH-4056 Basel, Switzerland

*Received October 19, 1995*[⊗]

The stabilization of unsupported Ti−M (M = Fe, Ru, Co) heterodinuclear complexes has been achieved by use of amidotitanium building blocks containing tripodal amido ligands. Salt metathesis of $H_3CC(CH_2NSiMe_3)_3TiX$ **(1)** and $C_6H_5C(CH_2NSiMe_3)_3TiX$ **(2)** as well as $HC\{SiMe_2N(4\text{-}CH_3C_6H_4)\}_3TiX$ **(3)** (X = Cl, **a**; Br, **b**) with $K[M(CO)_2Cp]$ (M = Fe, Ru) and $Na[Co(CO)_3(PR_3)]$ (R = Ph, Tol) gave the corresponding stable heterobimetallic complexes of which $H_3CC(CH_2NSiMe_3)_3Ti-M(CO)_2Cp$ (M = Fe, **6**; Ru, **7**) and $HC\{SiMe_2N(4\text{-}CH_3C_6H_4)\}_3Ti-M(CO)_2Cp$ (M = Fe, **12**; Ru, **13**) have been characterized by X-ray crystallography. **6**: monoclinic, $P2_1/n$, $a = 15.496(3)$ Å, $b = 12.983(3)$ Å, $c = 29.219(3)$ Å, $\beta = 104.52(2)°$, $Z = 8$, $V = 5690.71$ Å$^3$, $R = 0.070$. **7**: monoclinic, $P2_1/c$, $a = 12.977(3)$ Å, $b = 12.084(3)$ Å, $c = 18.217(3)$ Å, $\beta = 91.33(2)°$, $Z = 4$, $V = 2855.91$ Å$^3$, $R = 0.048$. **12**: monoclinic, $I2/c$, $a = 24.660(4)$ Å, $b = 15.452(3)$ Å, $c = 20.631(4)$ Å, $\beta = 103.64(3)°$, $Z = 8$, $V = 7639.65$ Å$^3$, $R = 0.079$. **13**: monoclinic, $I2/c$, $a = 24.473(3)$ Å, $b = 15.417(3)$ Å, $c = 20.783(4)$ Å, $\beta = 104.20(2)°$, $Z = 8$, $V = 7601.84$ Å$^3$, $R = 0.066$. $^1$H- and $^{13}$C-NMR studies in solution indicate free internal rotation of the molecular fragments around the Ti−M bonds. Fenske−Hall calculations performed on the idealized system $HC(CH_2NH)_3Ti-Fe(CO)_2Cp$ **(6x)** have revealed a significant degree of $\pi$-donor−acceptor interaction between the two metal fragments reinforcing the Ti−Fe $\sigma$-bond. Due to the availability of energetically low-lying $\pi$-acceptor orbitals at the Ti center this partial multiple bonding is more pronounced that in the tin analogue $HC(CH_2NH)_3Sn-Fe(CO)_2Cp$ **(15x)** in which an N−Sn $\sigma$*-orbital may act as $\pi$-acceptor orbital.

## Introduction

The past 3 decades have witnessed the characterization of an ever growing number of heterobimetallic complexes of the transition metals with unsupported metal−metal bonds.[1,2] However, the combination of metal complex fragments with significantly different electronic properties, such as those from opposite ends of the d-block of the periodic table, to form dinuclear systems may be difficult to achieve. Thus, in order to obtain such "early−late heterobimetallics" an additional (or even exclusive!) stabilization by bridging ligands has been employed in most cases, obscuring the role that the M−M′ bond plays in the structure (and reactivity) of these supported systems.[3]

It was not until the pioneering work in Selegue's group a decade ago that several Ti−M heterobimetallic complexes (M = Fe, Ru), containing unsupported Ti−M bonds, of the type $[(Me_2N)_3Ti-M(CO)_2Cp]$ could be structurally characterized.[4] Of these only the Ti−Ru species proved to be sufficiently stable to be studied in solution. More recently, Selent and coworkers synthesized a stable Ti−Co binuclear complex, $[(^tBuO)_3Ti-Co(CO)_4]$.[5] However, there has been no report of a general strategy for the synthesis of stable Ti−M complexes to date. Attempts to apply Casey's method for the preparation of $[Cp_2(R)Zr-M(CO)_2Cp]$[6] to the Ti-analogues failed due to the dominant single electron transfer (SET) which competes with the salt metathesis of metal carbonylates with {Ti−X} complexes.

In view of these observations, a general approach to the stabilization of Ti−M complexes (M = Fe, Ru, Co) has to take into account the following considerations for the choice of the appropriate Ti complex "building blocks":

(1) Reduction of the Ti-halide precursor complex by transition metal carbonylate derivatives (SET) should be suppressed by choice of an appropriate set of hard donor ligands.

(2) The electronic demand of the highly Lewis acidic Ti(IV)

[⊗] Abstract published in *Advance ACS Abstracts,* April 1, 1996.

(1) (a) Roberts, D. L.; Geoffroy, G. L. In *Comprehensive Organometallic Chemistry*; Wilkinson, G., Stone, F. G. A., Abel, E. W., Eds.; Pergamon Press: Oxford, England, 1982; Vol. 6, (b) Bruce, M. I. *J. Organomet. Chem.* **1983**, *242*, 147. (c) Bruce, M. I. *J. Organomet. Chem.* **1985**, *283*, 339.

(2) Herberhold, M.; Jin, G.-X. *Angew. Chem., Int. Ed. Engl.* **1994**, *33*, 964.

(3) (a) Stephan, D. W. *Coord. Chem. Rev.* **1989**, *95*, 41. (b) Bullock, R. M.; Casey, C. P. *Acc. Chem. Res.* **1987**, *20*, 167.

(4) (a) Sartain, W. S.; Selegue, J. P. *J. Am. Chem. Soc.* **1985**, *107*, 5818. (b) *Organometallics* **1987**, *6*, 1812. (c) *Organometallics* **1989**, *8*, 2153.

(5) Selent, D; Beckhaus, R.; Pickardt, J. *Organometallics* **1993**, *12*, 2857. The only other structurally characterized example of a compound containing an unsupported Ti−Co bond, $CpTi\{(\mu\text{-}CO)Co_3(CO)_9\}_2\{Co(CO)_4\}$, was reported by: Schmid, G.; Stutte, B.; Boese, R. *Chem. Ber.* **1978**, *111*, 1239.

(6) (a) Casey, C. P.; Jordan, R. F.; Rheingold, A. L. *J. Am. Chem. Soc.* **1983**, *105*, 665. (b) *Organometallics* **1984**, *3*, 504. (c) See also: Casey, C. P. *J. Organomet. Chem* **1990**, *400*, 205 and references cited therein.

0020-1669/96/1335-2433$12.00/0 

center should be met by using ligands which are both efficient $\sigma$- and $\pi$-donors.

(3) In order to effect kinetic and thermodynamic stabilization, the coordination of the ligands to the Ti center should be reinforced by integration into a common framework, i.e. using a polyfunctional ligand system.

These preconditions are ideally met by the Ti−amidohalide complexes containing the tripodal amido ligands which we have recently developed.[7,8] Preliminary studies have shown that they provide the key to the generation of stable Ti−M heterobimetallics.[9] In this paper we report the synthesis of a series of such dinuclear complexes and the single-crystal X-ray structure analyses of four of them. On the basis of the structural data obtained in this study, an analysis of the Ti−M bonding is given.

## Experimental Section

All manipulations were performed under an inert gas atmosphere of dried argon in standard (Schlenk) glassware which was flame dried with a Bunsen burner prior to use. Solvents were dried according to standard procedures and saturated with Ar. The deuterated solvents used for the NMR spectroscopic measurements were degassed by three successive "freeze−pump−thaw" cycles and dried over 4-Å molecular sieves.

The $^1$H-, $^{13}$C-, $^{29}$Si-, and $^{31}$P-NMR spectra were recorded on a Bruker AC 200 spectrometer equipped with a B-VT-2000 variable temperature unit (at 200.13, 50.32, 39.76, and 81.03 MHz, respectively) with tetramethylsilane and $H_3PO_4$ (85%, external) as references. Infrared spectra were recorded on Perkin-Elmer 1420 and Bruker IRS 25 FT-spectrometers.

Elemental analyses were carried out in the microanalytical laboratory of the chemistry department at Würzburg. The titanium complexes $H_3CC(CH_2NSiMe_3)_3TiBr$[8a] and $HC\{SiMe_2N(4\text{-}CH_3C_6H_4)\}_3TiBr$[8a] as well as the triamine $C_6H_5C(CH_2NHSiMe_3)_3$[10] were prepared as reported previously by us. The salts of the transition metal carbonylates K[CpFe(CO)$_2$], K[CpRu(CO)$_2$], Na[Co(CO)$_3$(PPh$_3$)], and Na[Co(CO)$_3$(PTol$_3$)] (Tol = 4-$CH_3C_6H_4$) were synthesized by literature methods.[11] All other chemicals used as starting materials were obtained commercially and used without further purification.

**(1) Preparation of $C_6H_5C(CH_2NSiMe_3)_3TiX$ (X = Cl, Br).** To a stirred solution of $C_6H_5C(CH_2NHSiMe_3)_3$ (1.82 g = 4.60 mmol) in 20 mL of *n*-pentane which was cooled at −40 °C were added 5.6 mL (13.8 mmol) of a 2.5 M *n*-butyllithium solution in hexanes. The reaction mixture was warmed to room temperature and subsequently refluxed for 10 min in order to effect complete lithiation. After recooling to −55 °C, solid $TiX_4(THF)_2$ (X = Cl, Br; 5.10 mmol) was added and the mixture warmed to ambient temperature over a period of 20 h. After removal of the LiX formed in the reaction by filtration through a G-3 frit, the solvent was completely removed *in vacuo* at $10^{-3}$ Torr. $C_6H_5C(CH_2NSiMe_3)_3TiX$ was obtained as a highly viscous dark red oil. The $^1$H-NMR spectra indicated the presence of ca. 5% impurities. This crude product was used in the subsequent metathetical coupling reactions. Attempts to purify **2a** and **2b** by distillation in high vacuum lead to partial thermal degration of the Ti complexes rather than a pure product. Satisfactory elemental analyses could thus not be obtained.

**Spectroscopic Data of $C_6H_5C(CH_2NSiMe_3)_3TiCl$ (2a).** Yield of the crude product: 84%. $^1$H-NMR (200.13 MHz, $C_6D_6$, 295 K): $\delta$ = 0.22 (s, 27 H, Si($CH_3$)$_3$), 3.99 (s, 6 H, $CH_2$N), 7.07−7.38 (m, 5 H, $C_6H_5$). {$^1$H}$^{13}$C-NMR (50.32 MHz, $C_6D_6$, 295 K): $\delta$ = 0.9 (Si($CH_3$)$_3$), 59.1 (Ph*C*), 62.4 ($CH_2$N), 125.6 (C$^3$), 127.3 (C$^4$), 129.1 (C$^2$), 145.4 (C$^1$). {$^1$H}$^{29}$Si-NMR (39.76 MHz, $C_6D_6$, 295 K): $\delta$ = 5.1.

**Spectroscopic Data of $C_6H_5C(CH_2NSiMe_3)_3TiBr$ (2b).** Yield of the crude product: 82%. $^1$H-NMR (200.13 MHz, $C_6D_6$, 295 K): $\delta$ = 0.25 (s, 27 H, Si($CH_3$)$_3$), 3.97 (s, 6 H, $CH_2$N), 7.13−7.38 (m, 5 H, $C_6H_5$). {$^1$H}$^{13}$C-NMR (50.32 MHz, $C_6D_6$, 295 K): $\delta$ = 1.3 (Si($CH_3$)$_3$), 59.7 (Ph*C*), 62.5 ($CH_2$N), 125.6 (C$^3$), 127.3 (C$^4$), 129.2 (C$^2$), 145.5 (C$^1$). {$^1$H}$^{29}$Si-NMR (39.76 MHz, $C_6D_6$, 295 K): $\delta$ = 0.9. IR (film): 3058 w, 3021 w, 2950 s, 2898 m, 2830 m, 1597 w, 1494 w, 1445 w, 1403 w, 1322 w, 1249 vs, 1128 m, 1065 s, 1019 s, 952 s, 840 vs, 751 s, 699 s, 656 m cm$^{-1}$.

**{$C_6H_5C[CH_2N(Li)SiMe_3]_3$}$_2$ (4).** The Li salt may be isolated by crystallization from pentane. Yield: 88%. Anal. Calcd for $C_{38}H_{76}Li_6N_6Si_6$: C, 55.17; H, 9.26; N, 10.16. Found: C, 55.38; H, 9.34; N, 9.94. $^1$H-NMR (200.13 MHz, $C_6D_6$, 295 K): $\delta$ = 0.25 (s, 27 H, Si($CH_3$)$_3$), 3.66 (s, 6 H, $CH_2$N), 6.99−7.63 (m, 5 H, $C_6H_5$). {$^1$H}$^{13}$C-NMR (50.32 MHz, $C_6D_6$, 295 K): $\delta$ = 1.3 (Si($CH_3$)$_3$), 51.8 (Ph*C*), 57.8 ($CH_2$N), 125.3 (C$^3$), 126.1 (C$^4$), 128.8 (C$^2$), 153.3 (C$^1$). {$^1$H}$^7$Li-NMR (77.77 MHz, $C_6D_6$, 295 K): $\delta$ = −0.06. {$^1$H}$^{29}$Si-NMR (39.76 MHz, $C_6D_6$, 295 K): $\delta$ = −2.3.

**(2) General Procedure for the Synthesis of the Heterodinuclear Complexes by Salt Metathesis.** A 1 mmol sample of solid alkali metal carbonylate was added to a solution of 1 mmol of **1b**, **2b**, or **3b** (**1b**, 458 mg; **2b**, 520 mg **3b**, 631 mg) in 30 mL of toluene which was cooled at −70 °C and the reaction mixture warmed to room temperature over a period of 20 h. Evaporation of the solvent, extraction of the residue with 20 mL of pentane and subsequent filtration yielded yellow-orange solutions of the heterobimetallic complexes. Evaporation of the solvent yielded the reaction products as microcrystalline solids which were washed with cold pentane. Single crystals suitable for X-ray crystallography were obtained by slow cooling of solutions of the compounds in toluene or diethyl ether.

**$H_3CC(CH_2NSiMe_3)_3Ti-Fe(CO)_2Cp$ (6).** Yield: 59%. Anal. Calcd for $C_{21}H_{41}FeN_3O_2Si_3Ti$: C, 45.40; H, 7.44; N, 7.56. Found: C, 45.16; H, 7.53; N, 7.60. $^1$H-NMR (200.13 MHz, $C_6D_6$, 295 K): $\delta$ = 0.41 (s, 27 H, Si($CH_3$)$_3$), 0.70 (s, 3 H, $CH_3$C), 3.10 (s, 6 H, $CH_2$N), 4.59 (s, 5 H, $C_5H_5$). {$^1$H}$^{13}$C-NMR (50.32 MHz, $C_6D_6$, 295 K): $\delta$ = 2.2 (Si($CH_3$)$_3$), 26.7 (*C*H$_3$C), 49.5 ($CH_3$*C*), 60.5 ($CH_2$N), 84.4 ($C_5H_5$), 216.6 (CO). {$^1$H}$^{29}$Si-NMR (39.76 MHz, $C_6D_6$, 295 K): $\delta$ = 2.5. IR (toluene): 2956 w, 2920 w, 1968 vs, 1916 vs, 1628 m, 1588 m, 1472 m, 1248 s, 1084 s, 1048 w, 920 w, 896 w, 848 vs cm$^{-1}$.

**$H_3CC(CH_2NSiMe_3)_3Ti-Ru(CO)_2Cp$ (7).** Yield: 68%. Anal. Calcd for $C_{21}H_{41}N_3O_2RuSi_3Ti$: C,41.98; H, 6.88; N, 6.99. Found: C, 41.93; H, 7.03; N, 6.98. $^1$H-NMR (200.13 MHz, $C_6D_6$, 295 K): $\delta$ = 0.40 (s, 27 H, Si($CH_3$)$_3$), 0.72 (s, 3 H, $CH_3$C), 3.14 (s, 6 H, $CH_2$N), 4.99 (s, $C_5H_5$). {$^1$H}$^{13}$C-NMR (50.32 MHz, $C_6D_6$, 295 K): $\delta$ = 2.3 (Si($CH_3$)$_3$), 26.5 (*C*H$_3$C), 50.3 ($CH_3$*C*), 60.6 ($CH_2$N), 87.2 ($C_5H_5$), 205.6 (CO). {$^1$H}$^{29}$Si-NMR (39.76 MHz, $C_6D_6$, 295 K): $\delta$ = 1.9. IR (*n*-hexane): 2948 vs, 2916 vs, 2896 vs, 2864 vs, 1988 s, 1932 vs, 1460 s, 1380 m, 1248 m, 1136 vw, 1008 vw, 984 w, 940 vw, 920 vw, 848 vs, 804 vw, 752 vw cm$^{-1}$.

**$H_3CC(CH_2NSiMe_3)_3Ti-Co(CO)_3(PPh_3)$ (8a).** Yield: 48%. Anal. Calcd for $C_{35}H_{51}CoN_3O_3PSi_3Ti$: C, 53.63; H, 6.56; N, 5.36. Found: C, 53.85; H, 7.00; N, 5.19. $^1$H-NMR (200.13 MHz, $C_6D_6$, 295 K): $\delta$ = 0.46 (s, 27 H, Si($CH_3$)$_3$), 0.85 (s, 3 H, $CH_3$C), 3.39 (s, 6 H, $CH_2$N), 6.96−7.09 (m, 15 H, P($C_6H_5$)$_3$). {$^1$H}$^{13}$C-NMR (50.32 MHz, $C_6D_6$, 295 K): $\delta$ = 1.3 (Si($CH_3$)$_3$), 26.4 (*C*H$_3$C), 50.2 ($CH_3$*C*), 61.5 ($CH_2$N), 128.6 (d, C$^3$, $^3J_{PC}$ = 10.3 Hz), 130.1 (C$^4$), 133.3 (d, C$^2$, $^2J_{PC}$ = 12.5 Hz), 135.5 (d, C$^1$, $^1J_{PC}$ = 39.7 Hz), 206.6 (CO, $^2J_{PC}$ not resolved). {$^1$H}$^{29}$Si-NMR (39.76 MHz, $C_6D_6$, 295 K): $\delta$ = 2.6. {$^1$H}$^{31}$P-NMR (81.03 MHz, $C_6D_6$, 295 K): $\delta$ = 56.0. IR (pentane): $\nu$ (CO) = 1930 vs cm$^{-1}$.

**$H_3CC(CH_2NSiMe_3)_3Ti-Co(CO)_3(PTol_3)$ (8b).** Yield: 44%. Anal. Calcd for $C_{38}H_{57}CoN_3O_3PSi_3Ti$: C, 55.26; H, 6.96; N, 5.09. Found: C, 55.47; H, 7.28; N, 5.18. $^1$H-NMR (200.13 MHz, $C_6D_6$, 295 K): $\delta$ = 0.50 (s, 27 H, Si($CH_3$)$_3$), 0.87 (s, 3 H, $CH_3$C), 1.98 (s, 9 H, C*H*$_3$C$_6$H$_4$), 3.40 (s, 6 H, $CH_2$N), 6.97 (d, 6 H, H$^3$, $^3J_{HH}$ = 7.8 Hz), 7.56 (d, 6 H, H$^2$). {$^1$H}$^{13}$C-NMR (50.32 MHz, $C_6D_6$, 295 K): $\delta$ = 1.4 (Si($CH_3$)$_3$), 21.1 ($CH_3C_6H_4$), 26.5 (*C*H$_3$C), 50.2 ($CH_3$*C*), 61.6 ($CH_2$N), 129.5 (d, C$^3$, $^3J_{PC}$ = 10.2 Hz), 132.7 (d, C$^1$, $^1J_{PC}$ = 41.6 Hz), 133.5 (d, C$^2$, $^2J_{PC}$

(7) (a) Gade, L. H.; Mahr, N. *J. Chem. Soc., Dalton Trans.* **1993**, 489. (b) Hellmann, K. W.; Gade, L. H.; Li, W.-S.; McPartlin, M. *Inorg. Chem.* **1994**, *33*, 5974. (c) Gade, L. H.; Becker, C.; Lauher, J. W. *Inorg. Chem.* **1993**, *32*, 2308.

(8) (a) Friedrich, S.; Gade, L. H.; Edwards, A. J.; McPartlin, M. *Chem. Ber.* **1993**, *126*, 1797. (b) Memmler, H.; Gade, L. H.; Lauher, J. W. *Inorg. Chem.* **1994**, *33*, 3064.

(9) Friedrich, S.; Memmler, H.; Gade, L. H.; Li, W.-S.; McPartlin, M. *Angew. Chem., Int. Ed. Engl.* **1994**, *33*, 676.

(10) Hellmann, K. W.; Friedrich, S.; Gade, L. H.; Li, W.-S.; McPartlin, M. *Chem. Ber.* **1995**, *128*, 29.

(11) (a) Brookhart, M.; Studabaker, W. B.; Husk, R. *Organometallics* **1987**, *6*, 1141. (b) Noak, K. *Helv. Chim. Acta* **1964**, *47*, 1555. (c) Manning, A. R. *J. Chem. Soc. A* **1968**, 1135. (d) Seyferth, D.; Millar, M. D. *J. Organomet. Chem.* **1972**, *38*, 373.

**Table 1.** Crystal Data and Experimental Details for **6**, **7**, **12**, and **13**

| | **6** | **7** | **12** | **13** |
|---|---|---|---|---|
| empirical formula | $C_{21}H_{41}FeN_3O_2Si_3Ti$ | $C_{21}H_{41}N_3O_2RuSi_3Ti$ | $C_{35}H_{45}FeN_3O_2Si_3Ti$ | $C_{35}H_{45}N_3O_2RuSi_3Ti$ |
| fw | 555.57 | 600.73 | 727.76 | 772.92 |
| cryst syst | monoclinic | monoclinic | monoclinic | monoclinic |
| cell params | | | | |
| *a* (Å) | 15.496(3) | 12.977(3) | 24.660(4) | 24.473(3) |
| *b* (Å) | 12.983(3) | 12.084(3) | 15.452(3) | 15.417(3) |
| *c* (Å) | 29.219(3) | 18.217(3) | 20.631(4) | 20.783(4) |
| $\beta$ (deg) | 104.52(2) | 91.33(2) | 103.64(3) | 104.20(4) |
| *V* (Å$^{3)}$ | 5690.71 | 2855.91 | 7639.65 | 7601.84 |
| Z | 8 | 4 | 8 | 8 |
| $D_{calc}$ (g cm$^{-3}$) | 1.297 | 1.397 | 1.265 | 1.351 |
| space group | $P2_1/n$ | $P2_1$/c | $I2/c$ | $I2/c$ |
| *F*(000) | 2352 | 1248 | 3056 | 3200 |
| $\mu$(Mo K$\alpha$) (cm$^{-1}$)[a] | 9.1 | 9.0 | 6.9 | 6.9 |
| $\theta$(max) (deg) | 25 | 25 | 21 | 25 |
| no. of reflcns $I > 3\sigma(I)$[b] | 2099 | 2903 | 1927 | 1904 |
| no. of variables[c] | 341 | 282 | 267 | 249 |
| residuals *R*; $R_w$[d] | 0.070; 0.072 | 0.048; 0.052 | 0.079; 0.079 | 0.066; 0.067 |
| data/parameter | 6.2 | 10.3 | 7.2 | 7.6 |

[a] An empirical absorption correction, using the program DIFABS (Walker, N.; Stuart, D. *Acta Crystallogr., Sect. A*, **1983**, *39*, 158) was applied to all four crystals; the data were corrected for Lorentz and polarization effects. [b] The intensities of three representative reflections were measured every 5 h of X-ray exposure time; they remained constant throughout the data collection indicating in every case crystal and electronic stability (no decay correction was applied). [c] Neutral atom scattering factors were taken from: Cromer, D. T.; Waber, J. T. *International Tables of X-ray Crystallography*; The Kynoch Press: Birmingham, England, 1974; Vol IV, Table 2.2A. Anomalous dispersion effects were included in the final $F_{calc}$ (Ibers, J. A.; Hamilton, W. C. *Acta Crystallogr.* **1964**, *17*, 781.). [d] $R = \sum||F_o| - |F_c||/\sum|F_o|$; $R_w = \sum||F_o| - |F_c||w^{1/2}/\sum|F_o|w^{1/2}$.

= 12.5 Hz), 140.2 (C$^4$), 207.2 (CO, $^2J_{PC}$ not resolved). {$^1$H}$^{29}$Si-NMR (39.76 MHz, $C_6D_6$, 295 K): $\delta$ = 2.5. {$^1$H}$^{31}$P-NMR (81.03 MHz, $C_6D_6$, 295 K): $\delta$ = 53.2. IR (pentane): 1932 vs, 1600 w, 1564 w, 1496 w, 1460 s, 1400 w, 1380 m, 1248 s, 1096 m, 1048 w, 1016 m, 984 w, 944 w, 924 m, 848 vs, 808 m, 756 w, 728 w cm$^{-1}$.

**$C_6H_5C(CH_2NSiMe_3)_3Ti-Fe(CO)_2Cp$ (9).** Yield: 32%. Anal. Calcd for $C_{26}H_{43}FeN_3O_2Si_3Ti$: C, 50.56; H, 7.02; N, 6.80. Found: C, 50.39; H, 7.08; N, 6.84. $^1$H-NMR (200.13 MHz, $C_6D_6$, 295 K): $\delta$ = 0.40 (s, 27 H, Si(CH$_3$)$_3$), 3.67 (s, 6 H, CH$_2$N), 4.60 (s, 5 H, C$_5$H$_5$), 6.99−7.37 (m, 5 H, C$_6$H$_5$). {$^1$H}$^{13}$C-NMR (50.32 MHz, $C_6D_6$, 295 K): $\delta$ = 2.4 (Si(CH$_3$)$_3$), 58.7 (Ph*C*), 60.6 (CH$_2$N), 84.2 (C$_5$H$_5$), 125.1 (C$^3$), 126.9 (C$^4$), 129.0 (C$^2$), 147.3 (C$^1$), 216.6 (CO). {$^1$H}$^{29}$Si-NMR (39.76 MHz, $C_6D_6$, 295 K): $\delta$ = 3.2. IR (toluene): 2890 vw, 2830 vw, 1958 vs, 1906 vs, 1400 vw, 1245 s, 1115 w, 1040 m, 995 w, 945 m, 885 m, 840 vs, 750 m, 650 m cm$^{-1}$.

**$C_6H_5C(CH_2NSiMe_3)_3Ti-Ru(CO)_2Cp$ (10).** Yield: 41%. Anal. Calcd for $C_{26}H_{43}N_3O_2RuSi_3Ti$: C, 47.11; H, 6.54; N, 6.34. Found: C, 47.22; H, 6.48; N, 6.36. $^1$H-NMR (200.13 MHz, $C_6D_6$, 295 K): $\delta$ = 0.38 (s, 27 H, Si(CH$_3$)$_3$), 3.71 (s, 6 H, CH$_2$N), 4.99 (s, 5 H, C$_5$H$_5$), 6.99−7.37 (m, 5 H, C$_6$H$_5$). {$^1$H}$^{13}$C-NMR (50.32 MHz, $C_6D_6$, 295 K): $\delta$ = 2.5 (Si(CH$_3$)$_3$), 59.4 (Ph*C*), 60.7 (CH$_2$N), 87.1 (C$_5$H$_5$), 125.2 (C$^3$), 127.0 (C$^4$), 129.1 (C$^2$), 147.1 (C$^1$), 205.6 (CO). {$^1$H}$^{29}$Si-NMR (39.76 MHz, $C_6D_6$, 295 K): $\delta$ = 2.6. IR (*n*-hexane): 1980 vs, 1925 vs, 1320 vw, 1250 s, 1115 vw, 1045 w, 995 w, 950 w, 845 vs, 805 m, 755 m, 698 m cm$^{-1}$.

**$C_6H_5C(CH_2NSiMe_3)_3Ti-Co(CO)_3(PPh_3)$ (11).** Yield: 23%. Anal. Calcd for $C_{40}H_{53}CoN_3O_3PSi_3Ti$: C, 56.79; H, 6.31; N, 4.97. Found: C, 56.38; H, 6.53; N, 4.81. $^1$H-NMR (200.13 MHz, $C_6D_6$, 295 K): $\delta$ = 0.47 (s, 27 H, Si(CH$_3$)$_3$), 3.97 (s, 6 H, CH$_2$N), 7.00−7.22, 7.45−7.63 (m, C$_6$H$_5$/P(C$_6$H$_5$)$_3$). {$^1$H}$^{13}$C-NMR (50.32 MHz, $C_6D_6$, 295 K): $\delta$ = 1.5 (Si(CH$_3$)$_3$), 59.4 (Ph*C*), 61.5 (CH$_2$N), 125.4 (Ph: C$^3$), 127.1 (Ph: C$^4$), 128.7 (d, PPh: C$^3$, $^3J_{PC}$ = 10.0 Hz), 129.2 (Ph: C$^2$), 130.2 (PPh: C$^4$), 133.4 (d, PPh: C$^2$, $^2J_{PC}$ = 12.4 Hz), 135.5 (d, PPh: C$^1$, $^1J_{PC}$ = 40.0 Hz), 146.9 (Ph: C$^1$), 202.4 (br, CO, $^2J_{PC}$ not resolved). {$^1$H}$^{29}$Si-NMR (39.76 MHz, $C_6D_6$, 295 K): $\delta$ = 3.3. {$^1$H}$^{31}$P-NMR (81.03 MHz, $C_6D_6$, 295 K): $\delta$ = 56.1. IR (pentane): 2880 br vs, 2725 m, 2660 w, 2610 w, 1923 s, 1455 vs, 1380 vs, 1340 s, 1325 m, 1305 m, 1260 s, 1140 s, 1095 m, 1070 m, 1025 s, 1010 s, 990 w, 915 s, 908 s, 865 s, 840 s, 765 s, 725 vs cm$^{-1}$.

**HC{$SiMe_2N(4\text{-}CH_3C_6H_4)$}$_3$Ti−Fe(CO)$_2$Cp (12).** Yield: 61%. Anal. Calcd for $C_{35}H_{45}FeN_3O_2Si_3Ti$: C, 57.77; H, 6.23; N, 5.77. Found: C, 58.03; H, 6.54; N, 5.43. $^1$H-NMR (200.13 MHz, $C_6D_6$, 295 K): $\delta$ = −0.78 (s, 1H, HC(Si...)$_3$), 0.33 (s, 18 H, Si(CH$_3$)$_2$), 2.21 (s, 9 H, 4-C*H*$_3$C$_6$H$_4$), 3.55 (s, 5 H, C$_5$H$_5$), 7.24 (d, 6 H, H$^2$, $^3J_{HH}$ = 8.2 Hz), 7.56 (d, 6 H, H$^3$). {$^1$H}$^{13}$C-NMR (50.32 MHz, $C_6D_6$, 295 K): $\delta$ = 4.0 (Si(CH$_3$)$_2$), 6.7 (HC(Si...)$_3$), 21.0 (4-*C*H$_3$C$_6$H$_4$), 85.3 (C$_5$H$_5$), 126.4 (C$^2$), 130.3 (C$^3$), 132.2 (C$^4$), 150.8 (C$^1$), 213.2 (CO). {$^1$H}$^{29}$Si-NMR (39.76 MHz, $C_6D_6$, 295 K): $\delta$ = 1.98. IR (benzene): 3020 w, 2958 w, 2920 w, 1975 vs, 1928 vs, 1604 w, 1511 m, 1496 vs, 1472 m, 1452 w, 1403 w, 1287 m, 1258 vs, 1244 vs, 1227 vs, 1172 m, 1104 m, 1018 m, 974 s, 942 m, 901 s, 892 s, 869 vs, 850 vs, 829 s, 811 vs, 742 w, 706 w, 649 w cm$^{-1}$.

**HC{$SiMe_2N(4\text{-}CH_3C_6H_4)$}$_3$Ti−Ru(CO)$_2$Cp (13).** Yield: 73%. Anal. Calcd for $C_{35}H_{45}N_3O_2Si_3TiRu$: C, 54.39; H, 5.87; N 5.42. Found: C, 54.10; H, 6.11; N, 5.24. $^1$H-NMR ($C_6D_6$, 295 K): $\delta$ = −0.68 (s, 1 H, HC(Si...)$_3$), 0.36 (s, 18 H, Si(CH$_3$)$_2$), 2.20 (s, 9 H, 4-C*H*$_3$C$_6$H$_4$), 4.07 (s, 5 H, C$_5$H$_5$), 7.23 (d, 6 H, H$^2$, $^3J_{HH}$ = 8.2 Hz), 7.52 (d, 6 H, H$^3$). {$^1$H}$^{13}$C-NMR (50.32 MHz, $C_6D_6$, 295 K): $\delta$ = 4.0 (Si(CH$_3$)$_2$), 7.1 (HC(Si...)$_3$), 20.9 (4-*C*H$_3$C$_6$H$_4$), 87.6 (C$_5$H$_5$), 126.1 (C$^2$), 130.0 (C$^3$), 132.2 (C$^1$), 149.5 (C$^4$), 202.8 (CO). {$^1$H}$^{29}$Si-NMR (36.76 MHz, $C_6D_6$, 295 K): $\delta$ = 2.6. IR (KBr): 3008 w, 2955 w, 2912 w, 1990 vs, 1932 vs, 1654 w, 1492 s, 1258 s, 1246 s, 1222 vs, 1102 m, 1015 m, 970 s, 918 w, 900 m, 890 m, 865 s, 843 vs, 825 s, 804 vs, 739 w, 700 w cm$^{-1}$.

**HC{$SiMe_2N(4\text{-}CH_3C_6H_4)$}$_3$Ti−Co(CO)$_3$(PPh$_3$) (14a).** Yield: 39%. Anal. Calcd for $C_{49}H_{55}CoN_3O_3PSi_3Ti$: C, 61.56; H, 5.80; N, 4.41. Found: C, 62.03; H, 5.65; N, 4.53. $^1$H-NMR (200.13 MHz, $C_6D_6$, 295 K): $\delta$ = −0.53 (s, 1 H, HC(Si...)$_3$), 0.43 (s, 18 H, Si(CH$_3$)$_2$), 2.28 (s, 9 H, 4-C*H*$_3$C$_6$H$_4$), 6.69−6.99 (m, 15 H, P(C$_6$H$_5$), 7.19 (d, 6 H, Tol: H$^2$, $^3J_{HH}$ = 8.0 Hz), 7.61 (d, 6 H, Tol-H$^3$). {$^1$H}$^{13}$C-NMR (50.32 MHz, $C_6D_6$, 295 K): $\delta$ = 4.2 (Si(CH$_3$)$_2$), 8.6 (HC(Si...)$_3$), 21.1 (4-*C*H$_3$C$_6$H$_4$), 125.7 (Tol: C$^2$), 129.3 (PPh: C$^4$), 129.4 (Tol: C$^3$), 129.8 (PPh; C$^3$), 132.0 (Tol: C$^4$), 133.4 (d, PPh: C$^2$, $^2J_{CP}$ = 12.2 Hz), 134.4 (d, PPh: C$^1$, $^1J_{CP}$ = 40.0 Hz), 150.5 (Tol: C$^1$), 205.1 (d, CO $^3J_{CP}$ = 16.4 Hz). {$^1$H}$^{29}$Si-NMR (36.76 MHz, $C_6D_6$, 295 K): $\delta$ = 3.8. {$^1$H}$^{31}$P-NMR (81.03 MHz, $C_6D_6$, 295 K): $\delta$ = 56.7. IR (benzene): 3050 w, 3012 w, 2643 w, 2003 w, 1938 vs, 1604 w, 1496 s, 1437 m, 1248 s, 1233 vs, 1174 w, 1098 w, 1093 m, 1018 w, 976 m, 942 w, 902 s, 869 vs, 847 vs, 812 s, 797 m, 755 m cm$^{-1}$.

**HC{$SiMe_2N(4\text{-}CH_3C_6H_4)$}$_3$Ti−Co(CO)$_3$(PTol$_3$) (14b).** Yield: 18%. Anal. Calcd for $C_{52}H_{61}CoN_3O_3PSi_3Ti$: C, 62.58; H, 6.16; N, 4.23. Found: C, 62.10; H, 6.01; N, 4.33. $^1$H-NMR (200.13 MHz, $C_6D_6$, 295 K): $\delta$ = −0.51 (s, 1 H, HC(Si...)$_3$), 0.45 (s, 18 H, Si(CH$_3$)$_2$), 1.93 (s, 9 H, 4-C*H*$_3$C$_6$H$_4$P), 2.31 (s, 9 H, 4-C*H*$_3$C$_6$H$_4$N), 6.81 −7.01 (m, 12 H, (Tol)$_3$P: H$^{2,3}$) 7.25 (d, 6 H, Tol: H$^2$, $^3J_{HH}$ = 8.0 Hz), 7.67 (d, 6 H, Tol: H$^3$). {$^1$H}$^{31}$P-NMR (81.03 MHz, $C_6D_6$, 295 K): $\delta$ = 53.6. IR (KBr): 3010 w, 2960 w, 2922 w, 2004 w, 1943 w, 1618 w, 1517 s,

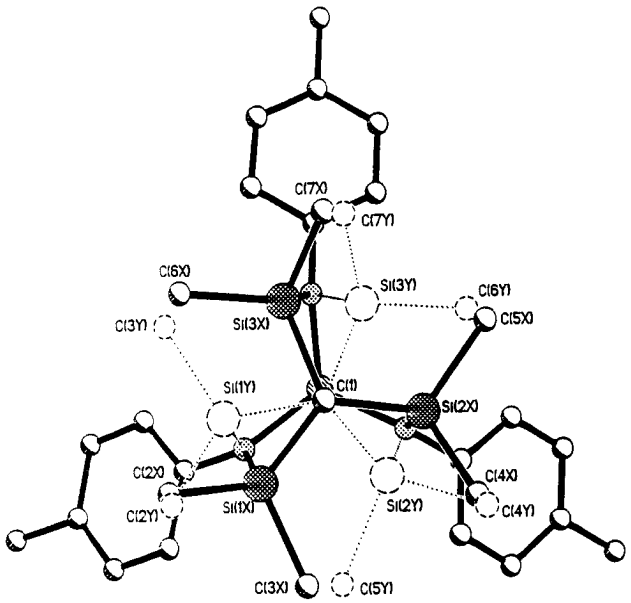


**Figure 1.** Molecular structure of **12** viewing down the Ti−Fe axis showing the two observed components of disorder, with the second set shown in dotted lines (the carbonyl and the cyclopentadienyl groups are omitted for clarity).

1499 s, 1288 w, 1258 s, 1231 m, 1179 w, 1098 s, 1021 s, 982 w, 906 s, 868 m, 847 s, 812 vs, 745 w, 713 w, 664 w $cm^{-1}$.

**X-ray Crystallographic Study of 6, 7, 12, and 13.** Yellow block-shaped crystals of **6** and **12** as well as clear orange crystals of **7** and **13** were mounted under argon in Lindemann capillaries. The X-ray diffraction data were collected using a Philips PW 1100 diffractometer with graphite-monochromated Mo Kα radiation. Unit cell parameters were determined by a least-squares analysis of 25 automatically centered reflections in the range of $10° < \theta < 15°$. Data were collected at 295 K in the range of $\theta = 3-25°$ with a scan width of 0.80° using a technique described previously.[12] Details are presented in Table 1.

The data analysis and refinement were carried out with the programs of the SHELX 76 software package. Crystals of **6** and **12** were difficult to obtain and diffracted only poorly. This resulted in relatively high standard deviations on all parameters, but the main features of the structures are well established. Initial refinement of the structure of **12** showed very high thermal parameters on the carbon and silicon atoms of the three dimethylsilyl groups. The silicon and carbon groups were resolved into two components corresponding to the presence of both twist helicities of the tripod ligand in the ratio 85:15 (Figure 1). Positions of the methyl carbons of the minor component were fixed in subsequent refinement and a common isotropic thermal parameter refined to 0.693 $Å^2$.

The coordinates of the metal atoms in all four structures were deduced from a Patterson synthesis. The remaining non-hydrogen atoms were located from subsequent difference Fourier syntheses and refined with anisotropic thermal parameters assigned to all non-hydrogen atoms. The positions of the hydrogen atoms were located in electron density difference maps and were included in the structure factor calculations with thermal factors of 0.08 $Å^2$, but their parameters not refined.

**Molecular Orbital Calculations.** Fenske−Hall calculations[13] were carried out on the model compounds $HC(CH_2NH)Ti-Fe(CO)_2Cp$ (**6x**) and $HC(CH_2NH)_3Sn$-$Fe(CO)_2Cp$ (**15x**) in terms of orbital interactions between the fragments $[HC(CH_2NH)_3Ti]^+$ and $[CpFe(CO)_2]^-$ as well as $[HC(CH_2NH)_3Sn]^+$ and $[CpFe(CO)_2]^-$. The coordinates determined in the crystal structures of **6** and $H_3CC(CH_2NSiMe_3)_3Sn$-$FeCp(CO)_2$ (**15**)[10] were used but with H-atoms replacing both the $Me_3Si$-groups bound to the amido-N atoms and the apical methyl group in the ligand framework. The calculations employed basis functions generated by the numerical Xα atomic orbital program of Herman and Skillman[14] used in conjunction with the Xα-to-Slater basis program of Bursten and Fenske.[15]

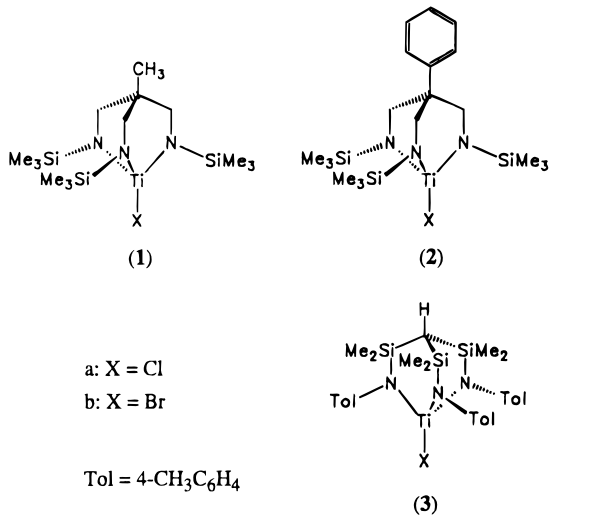


**Figure 2.** Ti building blocks for the synthesis of Ti−M heterodinuclear complexes **6**−**14**.

**Table 2.** Comparison of the $^1$H-NMR Chemical Shifts of the $CH_2-N$ Protons in the Ligand Frameworks $\{RC(CH_2NSiMe_3)_3\}$ (R = $CH_3$, $C_6H_5$) To Show the Ring Current Effect of an Apical Phenyl Group

| compound | δ(CH$_2$−N) | ref |
|---|---|---|
| R = $CH_3$ | | |
| $H_3CC(CH_2NSiMe_3)_3TiCl$ **(1a)** | 3.45 | 8a |
| $H_3CC(CH_2NSiMe_3)_3TiBr$ **(1b)** | 3.42 | 8a |
| $[H_3CC\{CH_2N(Li)SiMe_3\}_3]_2$ **(5)** | 3.23 | 7a |
| $H_3CC(CH_2NSiMe_3)_3Ti-Fe(CO)_2Cp$ **(6)** | 3.10 | this work |
| $H_3CC(CH_2NSiMe_3)_3Ti-Ru(CO)_2Cp$ **(7)** | 3.14 | |
| $H_3CC(CH_2NSiMe_3)_3Ti-Co(CO)_3(PPh_3)$ **(8a)** | 3.39 | |
| $H_3CC(CH_2NSiMe_3)_3Ti-Co(CO)_3(PTol_3)$ **(8b)** | 3.40 | |
| R = $C_6H_5$ | | |
| $C_6H_5C(CH_2NSiMe_3)_3TiCl$ **(2a)** | 3.99 | this work |
| $C_6H_5C(CH_2NSiMe_3)_3TiBr$ **(2b)** | 3.97 | |
| $[C_6H_5C\{CH_2N(Li)SiMe_3\}_3]_2$ **(4)** | 3.66 | |
| $C_6H_5C(CH_2NSiMe_3)_3Ti-Fe(CO)_2Cp$ **(9)** | 3.67 | |
| $C_6H_5C(CH_2NSiMe_3)_3Ti-Ru(CO)_2Cp$ **(10)** | 3.71 | |
| $C_6H_5C(CH_2NSiMe_3)_3Ti-Co(CO)_3(PPh_3)$ **(11)** | 3.97 | |

## Results and Discussion

**The Building Blocks.** The Ti building blocks for the synthesis of the heterodinuclear complexes by way of salt metathesis are displayed in Figure 2. The synthesis of compounds **1** and **3** has been previously reported and occurs by reaction of the completely lithiated triamine ligand precursor with $TiX_4(THF)_2$. The triamine $C_6H_5C(CH_2NHSiMe_3)_3$ has been used by us in the synthesis of tripodal triamidostannates[10] but has thus far not been applied in transition metal chemistry. The introduction of a phenyl group in the apical position of the ligand framework in **2** was thought to enhance the tendency of the heterobimetallics to crystallize from their reaction solutions. It is also to be seen in connection with a potential fixation of the tripod at a solid support material, an effort to be discussed elsewhere.

Reaction of the triamine $C_6H_5C(CH_2NHSiMe_3)_3$ with 3 molar equiv of *n*-BuLi in pentane yielded the trilithium salt **4**, which

(12) Cooper, M. K.; Guerney, P. J.; McPartlin, M. *J. Chem. Soc., Dalton Trans.* **1982**, 757.
(13) Hall, M. B.; Fenske, R. F. *Inorg. Chem.* **1972**, *11*, 768.
(14) Herman, F. and Skillman, S. *Atomic Structure Calculations*; Prentice Hall: Englewood Cliffs, NJ, 1963.
(15) (a) Bursten, B. E.; Fenske, R. F. *J. Chem. Phys.* **1977**, *67*, 3138. (b) Bursten, B. E.; Jensen, R. J.; Fenske, R. F. *J. Chem. Phys.* **1978**, *68*, 3320.

**Scheme 1.** Synthesis of the Ti−M Heterobimetallic Complexes **6**−**8** (a), **9**−**11** (b), and **12**−**14** (c) by Salt Metathesis of the Tripodal Amido Halides with Metal Carbonylates

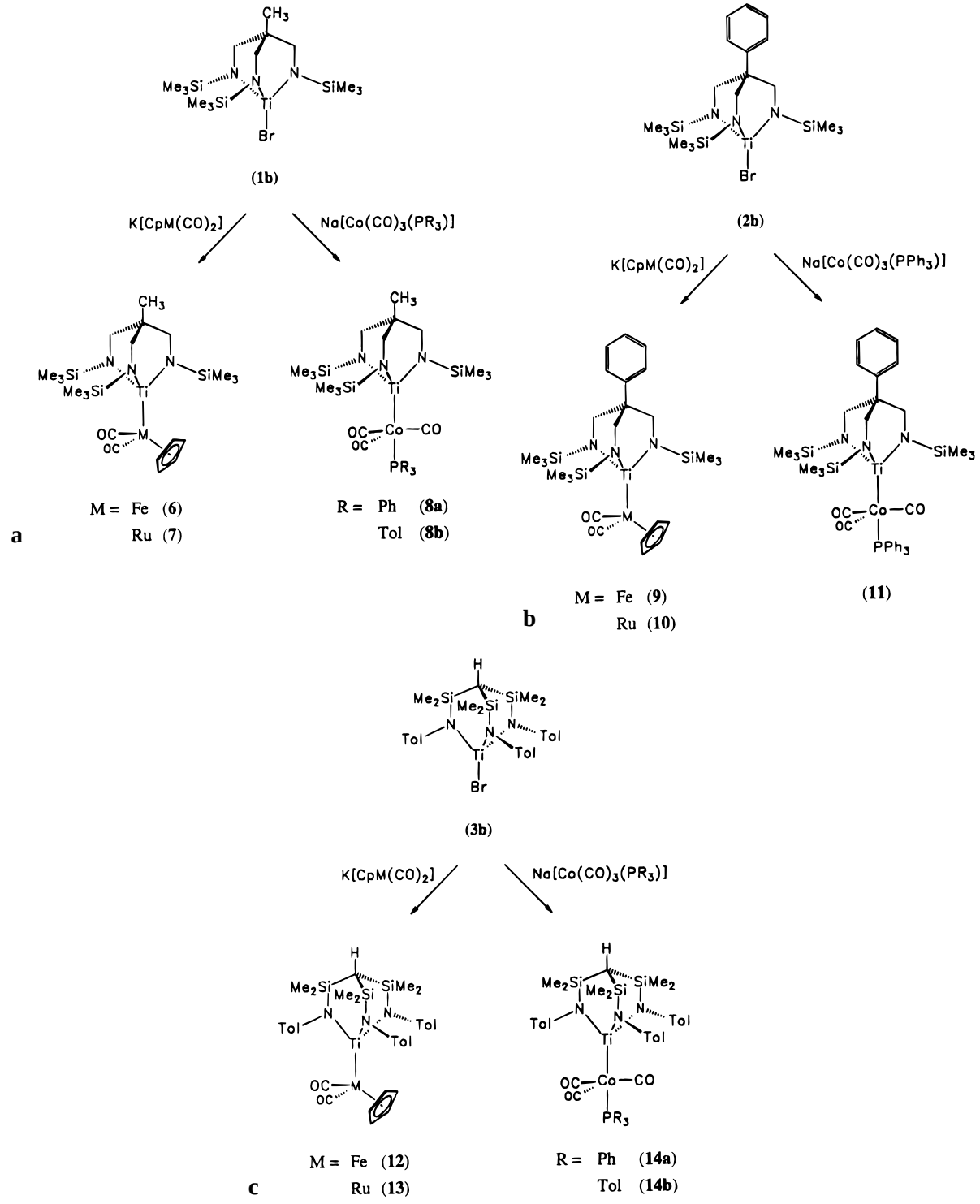


precipitated as a colorless solid and may be characterized as such. On the basis of a comparison of the NMR spectroscopic data to those of the previously characterized Li salts $[H_3CC\{CH_2N(Li)SiMe_3\}_3]_2$ (**5**) and $[H_3CC\{CH_2N(Li)(i\text{-}Pr)\}_3]_2$ of which X-ray crystal structures were obtained,[7a] a similar structural arrangement may be assumed for **4**. When **4** is reacted with $TiX_4(THF)_2$ the triamido−Ti complexes $C_6H_5C(CH_2NSiMe_3)_3TiX$ (X = Cl, **2a**; Br, **2b**) are obtained as red oils with a purity of approximately 95% based on $^1$H-NMR spectroscopy. Attempts to purify the titanium complexes by distillation at $10^{-3}$ Torr as previously achieved for **1a** and **1b** were unsuccessful since partial thermal degradation of the complexes actually led to additional contamination of the product. All attempts to crystallize **2a** and **2b** were equally unsuccessful. The crude amido complexes **2a** and **2b** were therefore employed in the subsequent metathetical coupling reactions.

A notable spectroscopic feature in the $^1$H-NMR spectra of **4**, **2a**, and **2b**, in comparison to their methyl-substituted analogues **5**, **1a**, and **1b**, respectively, is the downfield shift of the $CH_2N$ protons. This is thought to be a consequence of the ring current effect of the apical phenyl group in the former (Table 2).

**Synthesis of the Ti−M Heterobimetallic Complexes.** Reaction of the complexes **1b**, **2b**, or **3b** with carbonyl metallate derivatives according to Scheme 1 leads to the coupled

heterobimetallic, dinuclear complexes **6**−**8**, **9**−**11**, and **12**−**14**, respectively. The Ti−Fe complexes **6**, **9**, and **12** are the first compounds with an unsupported Ti−Fe bond which is stable in solution at ambient temperatures. In fact, **12** ist stable in toluene at 100 °C with decomposition only setting in after prolonged heating (boiling in toluene for several hours). Whereas **6** and **9** are moisture sensitive and decompose when exposed to oxygen, compound **12** is fairly stable to oxygen in the absence of moisture. In contrast to the thermally very stable Ti−Fe and Ti−Ru species, the Ti−Co complexes **8**, **11**, and **14** undergo slow thermal degradation if stirred in benzene or toluene over a period of several days (the degradation being complete only after weeks). In the course of the process the homodinuclear Co complexes $[Co(CO)_3(PR_3)]_2$ (R = Ph, Tol) precipitate from the solution; it has not been possible to date to establish the nature of the Ti components. More rapid decomposition occurs in polar solvents such as THF.

The existence of Ti−M bonds in **6**−**14** was initially evidenced by IR spectroscopy. The $\nu$(CO) bands of the heterobimetallics are shifted to higher wavenumbers relative to those of the alkali metal salts of the anions, as would be expected for metal−metal-bonded structures. As Fischer has pointed out[16] the shift to higher frequency $\Delta\nu(CO)_{as}$ of the asymmetric $^{12}C-O$ stretching vibration upon formation of the metal−metal bond may be used as a measure of the acceptor strength of the Lewis acidic metal fragment in relation to the base $[Cp(CO)_2M]^-$ (M = Fe, $\nu(CO)_{as}$ = 1770 $cm^{-1}$; M = Ru, $\nu(CO)_{as}$ = 1811 $cm^{-1}$ for the $K^+$ salt). The values of $\Delta\nu(CO)_{as}$ lie in the range 140−150 $cm^{-1}$, and the degree (if not necessarily the nature, *vide infra*) of donor−acceptor interaction is thus comparable to that observed for M−Ga-bonded dinuclear complexes.[17] Infrared absorptions attributable to bridging carbonyl or isocarbonyl ligands were observed for none of the compounds studied, which supports the structural arrangements depicted in Scheme 1.

Free rotation about the Ti−M bonds is inferred from the effective threefold symmetry of the titanium amide moiety observed in the NMR spectra. Whereas only a slight broadening of the $^1$H-NMR resonances assigned to the amido ligand is observed upon cooling solutions of **6**, **7**, **8**, and **9** in toluene-$d_8$ to 190 K, the amide signals in the spectra of **12** and **13** coalesce below 200 K. However, it proved impossible to reach the low temperature limit and thus freeze out the internal motion on the NMR time scale.

**X-ray Crystal Structure Analyses of 6 and 7.** Single-crystal X-ray structure analyses of **6** and **7** have established that while the compounds differ significantly with regard to their packing in the crystal and thus space group symmetry, their molecular structures are very similar. The crystals of **6**, in particular, were difficult to obtain and were weak diffractors. This resulted in relatively high standard deviations on all parameters, but the main features of the structure are well established. Since the unit cell of **6** contains two independent molecules, only the average values of the metric parameters will be discussed. The molecular structure of **6** in the crystal is shown in Figure 3, and the principal bond lengths and interbond angles are given in Table 3. A different view of the similar molecular structure of **7** is depicted in Figure 4, and the listing of the principal metric is given in Table 4.

The central structural unit is the free Ti−M bond (M = Fe, Ru) which is effectively shielded by the tripodal amido ligand

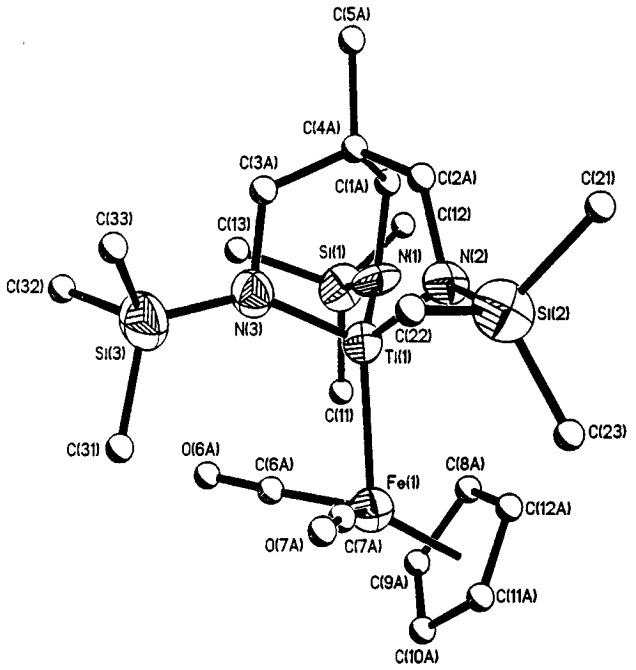


**Figure 3.** Molecular structure of the titanium−iron complex **6** (hydrogen atoms omitted for clarity).

**Table 3.** Principal Bond Lengths (Å) and Angles (deg) for **6**

| | | | | | |
|---|---|---|---|---|---|
| Molecule 1 | | | | | |
| Ti(1)−Fe(1) | 2.441(5) | Ti(1)−N(1) | 1.898(12) | Ti(1)−N(2) | 1.895(11) |
| Ti(1)−N(3) | 1.884(15) | Fe(1)−C(6a) | 1.72(2) | Fe(1)−C(7a) | 1.706(15) |
| N(1)−Si(1) | 1.734(12) | N(1)−C(1a) | 1.50(2) | N(2)−Si(2) | 1.740(11) |
| N(2)−C(2a) | 1.49(2) | N(3)−Si(3) | 1.73(2) | N(3)−C(3a) | 1.49(2) |
| C(6a)−O(6a) | 1.17(3) | C(7a)−O(7a) | 1.16(2) | | |
| N(1)−Ti(1)−Fe(1) | 113.5(4) | N(2)−Ti(1)−Fe(1) | 117.1(4) | | |
| N(2)−Ti(1)−N(1) | 105.6(6) | N(3)−Ti(1)−Fe(1) | 117.3(5) | | |
| N(3)−Ti(1)−N(1) | 99.8(6) | N(3)−Ti(1)−N(2) | 101.4(7) | | |
| C(6a)−Fe(1)−Ti(1) | 80.4(8) | C(7a)−Fe(1)−Ti(1) | 83.6(8) | | |
| C(7a)−Fe(1)−C(6a) | 98(1) | Si(1)−N(1)−Ti(1) | 138.6(8) | | |
| C(1a)−N(1)−Ti(1) | 104.9(9) | C(1a)−N(1)−Si(1) | 109(1) | | |
| Si(2)−N(2)−Ti(1) | 137.1(9) | C(2a)−N(2)−Ti(1) | 106.1(9) | | |
| C(2a)−N(2)−Si(2) | 107.9(9) | Si(3)−N(3)−Ti(1) | 144.5(9) | | |
| C(3a)−N(3)−Ti(1) | 105(1) | C(3a)−N(3)−Si(3) | 110(1) | | |
| O(6a)−C(6a)−Fe(1) | 176(2) | O(7a)−C(7a)−Fe(1) | 176(2) | | |
| Molecule 2 | | | | | |
| Ti(2)−Fe(2) | 2.428(5) | Ti(2)−N(4) | 1.891(11) | Ti(2)−N(5) | 1.879(12) |
| Ti(2)−N(6) | 1.89(2) | Fe(2)−C(6b) | 1.71(2) | Fe(2)−C(7b) | 1.71(2) |
| N(4)−Si(4) | 1.744(11) | N(4)−C(1b) | 1.50(2) | N(5)−Si(5) | 1.725(13) |
| N(5)−C(2b) | 1.49(2) | N(6)−Si(6) | 1.73(2) | N(6)−C(3b) | 1.49(3) |
| C(6b)−O(6b) | 1.16(2) | C(7b)−O(7b) | 1.16(3) | | |
| N(4)−Ti(2)−Fe(2) | 114.3(5) | N(5)−Ti(2)−Fe(2) | 114.9(5) | | |
| N(5)−Ti(2)−N(4) | 106.8(6) | N(6)−Ti(2)−Fe(2) | 117.8(5) | | |
| N(6)−Ti(2)−N(4) | 100.9(7) | N(6)−Ti(2)−N(5) | 100.3(6) | | |
| C(6b)−Fe(2)−Ti(2) | 82.0(8) | C(7b)−Fe(2)−Ti(2) | 84(1) | | |
| C(7b)−Fe(2)−C(6b) | 93(1) | Si(4)−N(4)−Ti(2) | 140.0(9) | | |
| C(1b)−N(4)−Ti(2) | 106(1) | C(1b)−N(4)−Si(4) | 107(1) | | |
| Si(5)−N(5)−Ti(2) | 139.7(9) | C(2b)−N(5)−Ti(2) | 103(1) | | |
| C(2b)−N(5)−Si(5) | 112(1) | Si(6)−N(6)−Ti(2) | 144.4(9) | | |
| C(3b)−N(6)−Ti(2) | 103(1) | C(3b)−N(6)−Si(6) | 111(1) | | |
| O(6b)−C(6b)−Fe(2) | 175(2) | O(7b)−C(7b)−Fe(2) | 175(2) | | |

at the Ti center as well as the set of ligands coordinated to the late transition metal. The average Ti−Fe distance of 2.433 Å in the structure of **6** and the Ti−Ru distance of 2.527(1) Å in that of **7** are significantly shorter than the corresponding bond lengths observed in $(Me_2N)_3Ti-M(CO)_2Cp$ [$d_{av}$(Ti−Fe) = 2.568, $d$(Ti−Ru) = 2.663(1) Å] and $(Me_2N)(2,6\text{-}Me_2C_6H_3O)_2$-Ti−Ru$(CO)_2$Cp [$d$(Ti−Ru) = 2.573(1) Å].[4] These short M−M′ bond distances are a consequence of the relatively high bond polarity as well as the low steric hindrance of the halves of the molecule. The possibility of a certain degree of metal−metal

(16) Fischer, R. A.; Priermeier, T. *Organometallics* **1994**, *13*, 4306 and references cited therein.

(17) (a) Burlitch, J. M.; Leonowicz, M. E.; Petersen, R. B.; Hughes, R. E. *Inorg. Chem.* **1978**, *18*, 1097. (b) Fischer, R. A.; Mier, A.; Priermeier, T. *Chem. Ber.* **1995**, *128*, 831.

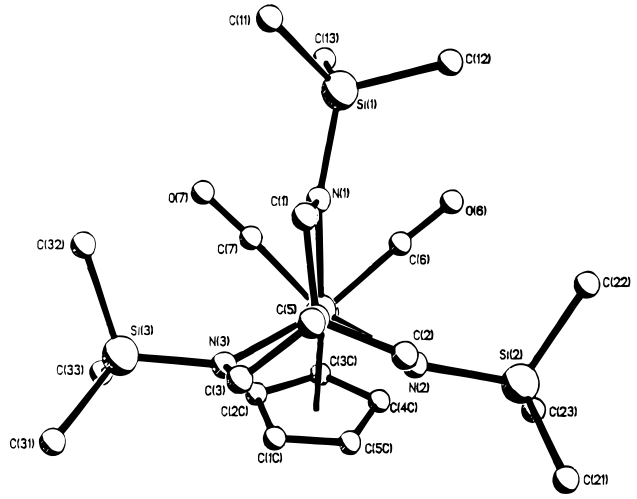


**Figure 4.** Molecular structure of **7** in the crystal showing the virtual $C_s$ symmetry of the molecule.

**Table 4.** Selected Bond Lengths (Å) and Angles (deg) for **7**

| | | | | | |
|---|---|---|---|---|---|
| Ru−Ti | 2.527(1) | Ti−N(1) | 1.907(5) | Ti−N(2) | 1.905(6) |
| Ti−N(3) | 1.907(6) | N(1)−Si(1) | 1.725(5) | N(2)−Si(2) | 1.732(6) |
| N(3)−Si(3) | 1.728(6) | N(1)−C(1) | 1.489(9) | N(2)−C(2) | 1.502(10) |
| N(3)−C(3) | 1.488(10) | C(4)−C(1) | 1.552(9) | C(4)−C(2) | 1.495(11) |
| C(4)−C(3) | 1.533(11) | C(4)−C(5) | 1.552(10) | Ru−C(6) | 1.840(9) |
| Ru−C(7) | 1.835(9) | C(6)−O(6) | 1.143(12) | C(7)−O(7) | 1.150(11) |

| | | | |
|---|---|---|---|
| N(1)−Ti−Ru | 118.1(2) | N(2)−Ti−Ru | 115.3(2) |
| N(3)−Ti−Ru | 113.1(2) | N(1)−Ti−N(2) | 102.0(3) |
| N(1)−Ti−N(3) | 100.1(2) | N(2)−Ti−N(3) | 106.4(2) |
| Si(1)−N(1)−Ti | 145.0(3) | C(1)−N(1)−Ti | 104.3(4) |
| C(1)−N(1)−Si(1) | 109.6(4) | Si(2)−N(2)−Ti | 140.2(4) |
| C(2)−N(2)−Ti | 105.1(5) | C(2)−N(2)−Si(2) | 109.3(5) |
| Si(3)−N(3)−Ti | 134.3(3) | C(3)−N(3)−Ti | 104.8(4) |
| C(3)−N(3)−Si(3) | 112.3(5) | C(6)−Ru−Ti | 79.6(3) |
| C(7)−Ru−Ti | 81.9(3) | C(7)−Ru−C(6) | 93.1(4) |
| O(6)−C(6)−Ru | 177.8(8) | O(7)−C(7)−Ru | 177.0(8) |

multiple bonding as invoked by Wolczanski et al. for the Zr−Rh complex $Cp^*Zr(\mu\text{-}OCH_2Ph_2P)_2RhMe_2$[18] will be discussed below.

In both compounds **6** and **7** the angle between the Cp(centroid)−M vector and the plane spanned by the metal (Fe, Ru) and the two carbonyl C-atoms, C(6) and C(7), is 160° in **6** and 163° in **7**, respectively and thus fairly close to the ideal value of 180° for the anion. This is typical for rather negatively charged metal centers in $Cp(CO)_2M^{\delta-}X^{\delta+}$ compounds.[19] The essentially linear carbonyl ligands lean markedly toward the Ti atoms [mean ∠(Ti−Fe−CO) 82.5° in **6**; mean ∠(Ti−Ru−CO) 80.8° in **7**]; however, the Ti···CO distance of about 2.8 Å in each compound precludes any "semibridging" interaction and indicates that the disposition of these ligands is largely determined by the steric requirements of the bulky cyclopentadienyl group.

Repulsion between the cyclopentadienyl ligand and the large N-bonded $Me_3Si$ groups at the other side of the Ti−Fe or Ti−Ru bond results in two silyl groups being forced apart (as can be seen in Figure 4), thus breaking the otherwise 3-fold symmetry of the Ti complex fragment. As a consequence of this distortion the geometry of the two amido-N atoms N(1) and N(2) in **6**; N(2) and N(3) in **7** significantly deviate from the normally observed planar arrangement [**6**: $\sum_{av}(\angle N(1)) = 353(1)°$, $\sum_{av}(\angle N(2)) = 353(1)°$; **7**: $\sum(\angle N(2)) = 354.6(5)°$, $\sum(\angle N(3)) = 351.4(5)°$].[20] The polydentate triamido ligand is clearly sufficiently flexible to accommodate these structural distortions without significant destabilization of the molecule.

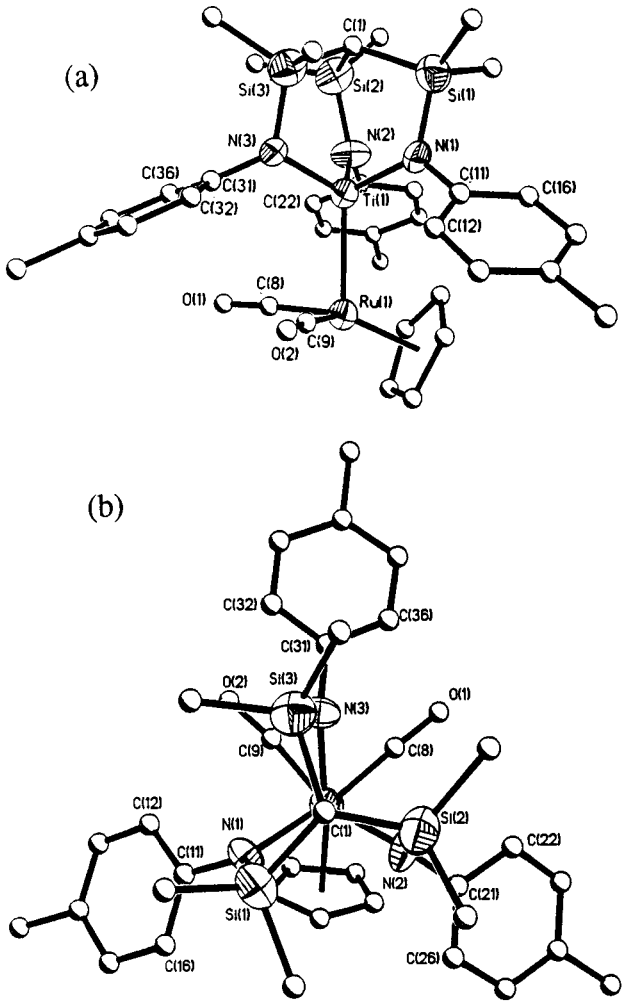


**Figure 5.** (a) Molecular structure of the titanium−ruthenium complex **13** showing the lampshade arrangement of the tripod ligand generated by the tolyl groups (complex **12** is virtually isostructural). (b) View down the Ti−Ru axis.

**X-ray Crystal Structure Analyses of 12 and 13.** The structural arrangement in the bimetallic complexes containing the trisilylmethane-derived tripodal amido ligand was established by single-crystal X-ray structure analyses of **12** and **13**. The molecular structures of both compounds are closely related and depicted in Figure 5. The principal bond lengths and interbond angles of both compounds are given in Tables 5 and 6. The dominant structural feature is the [2,2,2]bicyclooctane-derived cage comprising the trisilylmethane unit and the tris(amido)-titanium unit which are slightly twisted with respect to each other as a consequence of the steric repulsion of the $SiMe_2$ groups. In the crystals obtained from **12** there is a slight disorder of the $SiMe_2$ units due to the presence of both twist-helicities of the tripodal ligand in a ratio of approx. 85:15.

The tolyl groups are oriented almost orthogonally to the radial planes spanned by the Ti, N, and Si atoms [torsion angles: **12**, ∠(Si(1*x*)−N(1)−C(11)−C(12)) = −54.3°, ∠(Si(2x)−N(2)−C(21)−C(22)) = −84.7°, ∠(Si(3x)−N(3)−C(31)−C(32)) = −69.4°; **13**, ∠(Si(1)−N(1)−C(11)−C(16)) = −55.2°, ∠(Si(2)−N(2)−C(21)−C(22)) = −84.8°, ∠(Si(3)−N(3)−C(31)−C(32))

(18) Ferguson, G. S.; Wolczanski, P. T.; Parkanyi, L.; Zonnevylle, M. C. *Organometallics* **1988**, *7*, 1967.
(19) Fischer, R. A.; Herdtweck, E.; Priermeier, T. *Inorg. Chem.* **1994**, *33*, 934 and references cited therein.
(20) Chisholm, M. H.; Rothwell, I. P. In *Comprehensive Coordination Chemistry* Wilkinson, G., McCleverty, J. A., Gillard, R. D., Eds.; Pergamon Press: Oxford, England, 1987; Vol. 2, p 161.

**Table 5.** Selected Bond Lengths (Å) and Angles (deg) for **12**

| | | | | | |
|---|---|---|---|---|---|
| Ti−Fe | 2.410(4) | Ti−N(1) | 1.942(10) | Ti−N(2) | 1.915(10) |
| Ti−N(3) | 1.929(11) | Fe−C(8) | 1.731(15) | Fe−C(9) | 1.71(2) |
| Si(1*x*)−N(1) | 1.781(12) | N(1)−Si(1*y*) | 1.79(3) | N(1)−C(11) | 1.43(2) |
| Si(2*x*)−N(2) | 1.777(12) | N(2)−Si(2*y*) | 1.79(3) | N(2)−C(21) | 1.42(2) |
| Si(3*x*)−N(3) | 1.771(13) | N(3)−Si(3*y*) | 1.79(2) | N(3)−C(31) | 1.44(2) |
| O(1)−C(8) | 1.16(2) | O(2)−C(9) | 1.16(2) | | |

| | | | |
|---|---|---|---|
| N(1)−Ti−Fe | 115.5(3) | N(2)−Ti−Fe | 113.1(4) |
| N(2)−Ti−N(1) | 104.3(5) | N(3)−Ti−Fe | 116.3(4) |
| N(3)−Ti−N(1) | 102.6(5) | N(3)−Ti−N(2) | 103.5(5) |
| C(8)−Fe−Ti | 88.0(6) | C(9)−Fe−Ti | 88.8(6) |
| C(9)−Fe−C(8) | 96.8(8) | C(11)−N(1)−Ti | 125.2(9) |
| C(11)−N(1)−Si(1*x*) | 120.6(9) | C(11)−N(1)−Si(1*y*) | 112(1) |
| C(21)−N(2)−Ti | 129(1) | C(21)−N(2)−Si(2*x*) | 116.1(9) |
| C(21)−N(2)−Si(2*y*) | 114(1) | C(31)−N(3)−Ti | 129(1) |
| C(31)−N(3)−Si(3*x*) | 118(1) | C(31)−N(3)−Si(3*y*) | 116(1) |
| O91)−C(8)−Fe | 176(2) | O(2)−C(9)−Fe | 177(2) |

**Table 6.** Selected Bond Lengths (Å) and Angles (deg) for **13**

| | | | | | |
|---|---|---|---|---|---|
| Ti(1)−Ru(1) | 2.503(4) | Ti(1)−N(1) | 1.932(11) | Ti(1)−N(2) | 1.902(14) |
| Ti(1)−N(3) | 1.895(13) | N(1)−Si(1) | 1.754(15) | N(2)−Si(2) | 1.74(2) |
| N(3)−Si(3) | 1.73(2) | Si(1)−C(1) | 1.88(2) | Si(1)−C(2) | 1.84(2) |
| Si(1)−C(3) | 1.89(2) | Si(2)−C(1) | 1.84(2) | Si(2)−C(4) | 1.90(2) |
| Si(2)−C(5) | 1.88(2) | Si(3)−C(1) | 1.89(2) | Si(3)−C(6) | 1.87(2) |
| Si(3)−C(7) | 1.86(2) | N(1)−C(11) | 1.43(2) | N(2)−C(21) | 1.43(2) |
| N(3)−C(31) | 1.43(2) | C(8)−O(1) | 1.15(2) | C(9)−O(2) | 1.17(3) |
| Ru(1)−C(8) | 1.81(2) | Ru(1)−C(9) | 1.80(2) | | |

| | | | |
|---|---|---|---|
| N(1)−Ti(1)−Tu(1) | 113.9(4) | N(2)−Ti(1)−Ru(1) | 112.7(5) |
| N(3)−Ti(1)−Ru(1) | 117.7(5) | N(2)−Ti(1)−N(1) | 103.9(6) |
| N(3)−Ti(1)−N(1) | 102.7(6) | N(3)−Ti(1)−N(2) | 104.5(6) |
| Si(1)−N(1)−Ti(1) | 113.3(7) | C(11)−N(1)−Ti(1) | 125(1) |
| C(11)−N(1)−Si(1) | 121(1) | Si(2)−N(2)−Ti(1) | 113.8(7) |
| C(21)−N(2)−Ti(1) | 128(1) | C(21)−N(2)−Si(2) | 118(1) |
| Si(3)−N(3)−Ti(1) | 113.6(7) | C(31)−N(3)−Ti(1) | 129(1) |
| C(31)−N(3)−Si(3) | 118(1) | C(9)−Ru(1)−C(8) | 91.2(8) |
| Ti(1)−Ru(1)−C(8) | 87.8(7) | Ti(1)−Ru(1)−C(9) | 88.4(8) |
| O(1)−C(8)−Ru(1) | 177(2) | O(2)−C(9)−Ru(1) | 173(2) |
| C(1)−Si(1)−N(1) | 102.0(7) | C(1)−Si(2)−N(2) | 102.9(7) |
| C(1)−Si(3)−N(3) | 103.1(7) | Si(1)−C(1)−Si(2) | 112.7(9) |
| Si(1)−C(1)−Si(3) | 110.6(9) | Si(2)−C(1)−Si(3) | 112.1(8) |

$= -71.9°$] generating a lamp shade arrangement of the ligand which leaves sufficient space for the Fe and Ru fragments to bind to the Ti without significant steric repulsion of the two complex fragments. This is also manifested in the extremely short metal−metal bonds [$d$(Ti−Fe) = 2.410(4) Å, $d$(Ti−Ru) = 2.503(4) Å] which are even shorter than those observed in **6** and **7**.

That the arrangement of the tolyl groups observed in the solid state structures of **12** and **13** is retained in solution is inferred from the shift of the Cp protons in the $^1$H-NMR spectra of both compounds to higher field. [$\delta$ = 3.55 (**12**), 4.07 (**13**) in comparison to $\delta$ 4.59 (**6**) 4.99 (**7**)]. The significant shift to higher field is due to the ring current effects of the tolyl groups, the Cp ligands lying within the high field shifting anisotropy cones of the arene rings.

**Analysis of the Metal−Metal Bonding in HC(CH$_2$NH)$_3$Ti−Fe(CO)$_2$Cp (6x) and HC(CH$_2$NH)$_3$Sn−Fe(CO)$_2$Cp (15x).** The unusually short metal−metal bonds found in the crystal structures of **6**, **7**, **12**, and **13** have raised the question of the actual bond multiplicity in these early−late heterobimetallics. An early theoretical study of Cp(I)Zr−RuCp(CO)$_2$ by Bursten and Novo-Gradac revealed a certain degree of $\pi$-donor−acceptor interaction between the metal centers.[21] In analogy to the qualitative view adopted by Wolczanski and coworkers in their analysis of the Zr−Rh bonding in Cp*Zr($\mu$-OCH$_2$Ph$_2$P)$_2$-RhMe$_2$[18] the compounds discussed in this paper may be viewed as arising from a $\sigma$- and $\pi$-donor−acceptor interaction between an anionic [CpM(CO)$_2$]$^-$ fragment and the cationic [(Amide)-Ti]$^+$ fragment. To elucidate the detailed nature of Ti−M bonding in these species, Fenske−Hall quantum mechanical calculations on the model compound HC(CH$_2$NH)$_3$Ti−Fe(CO)$_2$Cp (**6x**) were carried out. The coordinates of the crystal structure of **6** were used, the N-bonded Me$_3$Si groups and the methyl group in the ligand framework being replaced by H-atoms. The analysis of the results is considered in terms of the interaction between the fragments [HC(CH$_2$NH)$_3$Ti]$^+$ and [CpFe(CO)$_2$]$^-$ (Figure 6).

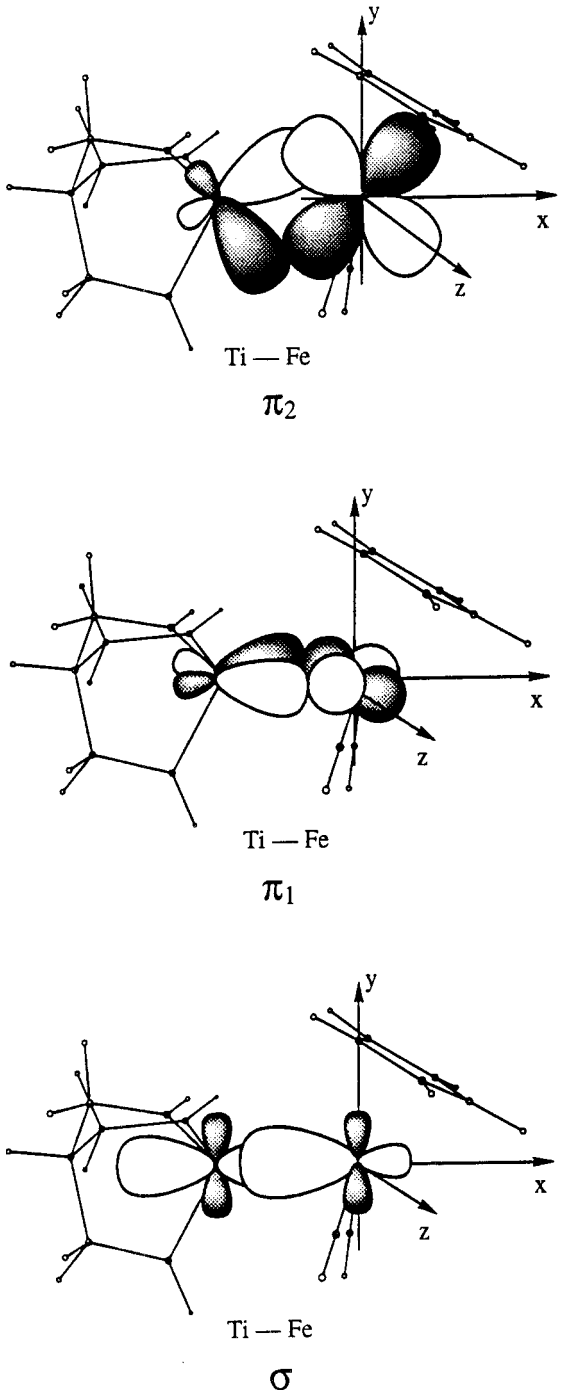


**Figure 6.** $\sigma$-donor and two $\pi$-donor acceptor orbital interactions between [HC(CH$_2$NH)$_3$Ti]$^+$ and [CpFe(CO)$_2$]$^-$ in **6x**.

There are three principal donor−acceptor bonding interactions between these two fragments, one dominant $\sigma$-bonding interaction and two orthogonal $\pi$-interactions ($\pi_1$ and $\pi_2$). Mulliken overlap population (MOP) analysis of these bonding interactions (Table 7) indicates that the $\sigma$-interaction between acceptor fragment orbital 23 of the Ti$^+$ unit, MO(Ti) 23, and donor fragment orbital 27 (the HOMO) of the Fe$^-$ unit, MO(Fe) 27,

(21) Bursten, B. E.; Novo-Gradac, K. J. *J. Am. Chem. Soc.* **1987**, *109*, 904.

**Table 7.** Mulliken Overlap Populations Between the Fragments $[HC(CH_2NH)_3Ti]^+$ and $[CpFe(CO)_2]^-$

| fragment MOs in $[HC(CH_2NH)_3Ti]^+$ | fragment MOs in $[CpFe(CO)_2]^-$ | | | |
|---|---|---|---|---|
| | 24 | 25 | 26 | 27 |
| 23 | | | | 0.327 (67%) |
| 24 | 0.022 (4.5%) | | 0.037 (8%) | |
| 25 | | 0.100 (20.5%) | | |

accounts for 67% of the metal−metal bonding. The $\pi_1$-orbital interaction between MO(Ti) 25 and MO(Fe) 25 is responsible for 20.5% while $\pi_2$ accounts for 8% of the molecular overlap population between the two metals. A residual MOP of 0.022 is in the interaction of MO(Ti) 24 and MO(Fe) 24, which is not shown in Figure 6. To summarize, the Ti−Fe bonding in **6x** is predominantly of the $\sigma$-donor−acceptor type, however with a significant component of $\pi$-bonding also involved.

In order to compare the nature of the Ti−M bonding with that of the metal metal bonding in the tetravalent main group analogues, we recently synthesized the analogous Sn−M heterobimetallics.[10] Of these, the complex $H_3CC(CH_2NSiMe_3)_3$-Sn−Fe$(CO)_2$Cp (**15**) represents the tin analogue of **6**. Using the crystallographically determined coordinates of **15** and replacing the $SiMe_3$ and (ligand framework) methyl groups by H-atoms, we performed similar calculations to those discussed above on the model compound $HC(CH_2NH)_3$Sn−Fe$(CO)_2$Cp (**15x**). As in the analysis of **6x**, the bonding in this compound was considered in terms of the orbital interactions between the $[HC(CH_2NH)_3Sn]^+$ and $[CpFe(CO)_2]^-$ fragments (Figure 7).

There are two principal donor acceptor interactions between the two complex fragments, the dominant interaction being the $\sigma$-bond between MO(Fe) 27 and MO(Sn) 28. This type of interaction which is analogous to the $\sigma$-bonding interaction in **6x** accounts for 74% of the Fe−Sn bonding (MOP 0.517). In addition, a donor−acceptor $\pi$-bond arising from the interaction of MO(Fe) 25 with MO(Sn) 29 contributes significantly to the bonding between Fe and Sn (MOP 0.124 amounting to 18% of the total Fe−Sn bonding). The $\pi$-bonding is due to the interaction between the $d_{xy}$ orbital of the Fe-fragment and a Sn−N $\sigma$*-orbital of the tin fragment. Since the Sn−N bonding is essentially ionic ($Sn^+-N^-$) in nature, this orbital is predominantly of Sn character (76%).

To summarize, while there are two possible $\pi$-donor−acceptor metal−metal interactions in the Ti−Fe complex due to the availablity of low lying acceptor d-orbitals in the early transition metal, the Fe−Sn $\pi$-bonding involves an essentially Sn-centered Sn−N $\sigma$*-orbital. For the stabilization of the metal−metal bond this interaction is clearly less dominant than the $\pi$-bonding in **6x**. The more "conventional" Sn−Fe metal−metal bond is therefore to be interpreted as primarily a $\sigma$-bond.

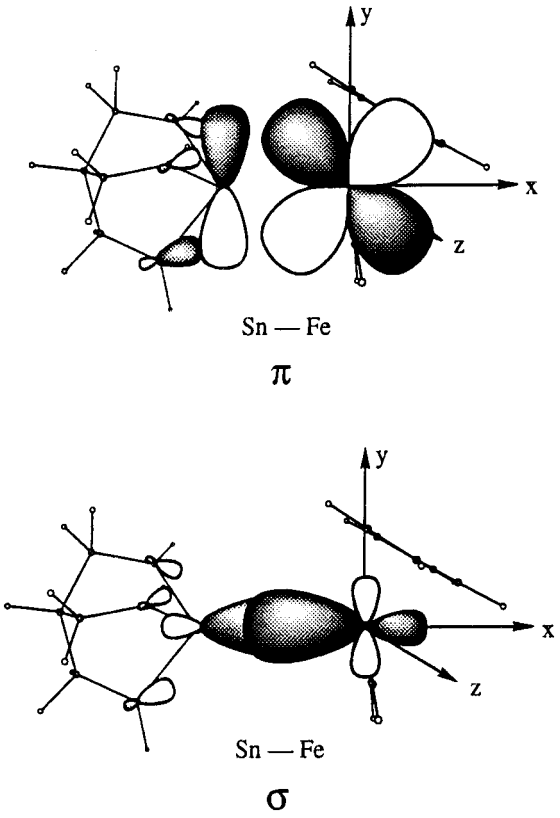


**Figure 7.** Major frontier orbital interactions in **15x**.

## Conclusions

The choice of the tripodal amido ligands in the stabilization of Ti−M heterobimetallics has provided the key to the synthesis of a whole range of such species. This study has shown that by use of an appropriately "protected" early transition metal complex fragment polar metal−metal bonds in early−late heterobimetallics are stable structural elements. In current and future work we are investigating the chemical and photochemical reactivity of these dinuclear systems.

**Acknowledgment.** We thank the Deutsche Forschungsgemeinschaft, the Fonds der Chemischen Industrie, the EPSRC, the DAAD, and the British Council (ARC 313 grant to L.H.G. and M.M.) for financial support and Degussa AG as well as Wacker Chemie AG for generous gifts of basic chemicals. Thanks is also due to Professor H. Werner (Würzburg, Germany) for his continued interest and support of this work.

**Supporting Information Available:** Text detailing the structure determination, tables of crystallographic data, the positional and thermal parameters, and interatomic distances and angles, and structural diagrams for **6**, **7**, **12** and **13** (42 pages). Ordering information is given on any masthead page.

IC951353F